Jurnal Tribologi 49 (2026) 1-13

MYTRIBOS Malaysian Tribology Society

Jurnal Tribologi

Website : jurnaltribologi.mytribos.org e-issn: 2289-7232

Numerical study on hydrodynamic pressure characteristics of journal bearings: Role of L/D ratio and surface texturing

Nadia Nurul Nabihah Ahmad Fuad [1], Mohamad Ali Ahmad [1*], Salmiah Kasolang [1], Jaharah A. Ghani [3]

[1] Tribology for Transportation Industry (Center of Tribology), Faculty of Mechanical Engineering, Universiti Teknologi MARA, Jalan Ilmu 1/1, 40450, Shah Alam, MALAYSIA.
[2] Jabatan Kejuruteraan Mekanikal & Pembuatan, Universiti Kebangsaan Malaysia, Lingkungan Ilmu, 43600, Bangi, MALAYSIA.
*Corresponding author: mohama9383@uitm.edu.my

KEYWORDS

Length-to-diameter ratio
CFD analysis
Coupling system simulation
Pressure profile
Dimple depth

ABSTRACT

The performance of journal bearings is primarily influenced by geometric characteristics that impact pressure capacity and load-carrying ability. The geometry of bearings and surface texturing are crucial for optimising bearing design and enhancing lubrication efficiency. This study evaluates the effects of the length-to-diameter (L/D) ratio and dimple depth on the hydrodynamic performance of journal bearings using numerical analysis. Simulations were performed between smooth and textured bearing surfaces incorporating circular, elliptical, and square dimples at a rotational speed of 300 rpm and at loads of 10 and 20 kN, on two bearing length ratios (L/D = 0.5 and 1.0). The results reveal that surface texturing modifies the pressure distribution within the lubricant film. The circular dimple design had lower pressure readings than the plain and other textured surfaces, which improved the frictional resistance between surfaces to reduce heat generation and enhance system efficiency. This study also highlights the importance of dimple depth that improved hydrodynamic pressure and film stability. Excessive depths can disturb the pressure field and increase the likelihood of cavitation. Overall, the findings demonstrate that optimising dimple geometry and the L/D ratio can significantly enhance hydrodynamic bearing performance by improving pressure capacity and promoting more stable lubrication conditions.

Received 31 August 2025; received in revised form 31 December 2025; accepted 28 January 2026.
To cite this article: Ahmad Fuad et al. (2026). Numerical study on hydrodynamic pressure characteristics of journal bearings: Role of L/D ratio and surface texturing. Jurnal Tribologi 49, pp.1-13.

1.0 INTRODUCTION

Journal bearings were a critical component in rotary machines that provide load support. The performance of journal bearings is strongly influenced by geometric and operating parameters, including clearance, eccentricity ratio, rotational speed, lubricant viscosity, and bearing length, as shown in Figure 1. Among these, the length-to-diameter ratio (L/D) has a significant effect on the hydrodynamic pressure distribution, load-carrying capacity, and overall stability of the bearing system (Marey, 2019; Sharma and Awasthi, 2018).

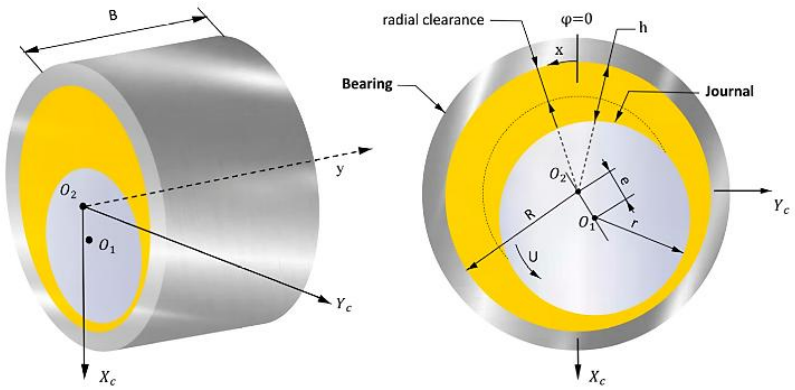

Figure 1: Hydrodynamic journal bearing schematic (Kong et al., 2025).

where, O_1 is the journal centre, O_2 is the bearing centre, e is the shaft eccentricity ratio, r is the journal radius, R is the bearing radius, U is the rotational speed, X_c and Y_c are translational coordinates, X and y are angular coordinate, and B is bearing width/length.

In general, short bearings (low L/D ratio) generate lower peak pressures but provide more uniform pressure distribution across the surface. This results in reduced sensitivity to misalignment and greater load support per unit length, making them suitable for high-load applications. Conversely, long bearings (high L/D ratio) can sustain higher hydrodynamic pressures but tend to develop steeper pressure gradients along the circumferential direction. These conditions can increase the risk of localised stress concentrations, vibration, and wear at specific regions of the bearing surface.

Previous studies have extensively analysed the impact of bearing length on hydrodynamic performance. Classical hydrodynamic theory, as presented by Reynolds and further extended in modern analyses, shows that the pressure profile and film thickness strongly depend on the L/D ratio. Numerical studies demonstrated that shorter bearings exhibit more stable lubrication regimes, whereas longer bearings often experience higher eccentricity effects and non-uniform load distribution (Y. Liu et al., 2021). Experimental investigations have also confirmed that the stability threshold of a bearing is directly linked to its aspect ratio, with longer bearings being more prone to instability under dynamic loading conditions.

More recent computational studies have further validated these trends. Khonsari and Booser, 2017 highlighted that an optimal L/D ratio must be selected to balance load-carrying capacity and operational stability. Too short a bearing results in excessive leakage and reduced pressure build-up, while too long a bearing may cause excessive peak pressures that lead to localised wear. Thus, the choice of bearing length remains a critical consideration for design, particularly when

combined with surface modifications such as texturing or the inclusion of dimples to enhance hydrodynamic effects.

Researchers have demonstrated that the addition of micro-dimples, among other approaches, affects load capacity, pressure distribution, friction, and wear behaviour. Several studies have shown that texturing does not necessarily offer benefits when applied indiscriminately. For example, authors (Kligerman et al., 2005; Cohen and Goltsberg, 2023) discovered that partial texturing can provide benefits equivalent to Rayleigh step bearings. However, full texturing may degrade performance. Similarly, Tala-Ighil et al., 2011 found that a strategic distribution of textured zones improved hydrodynamic load capacity more than entire coverage.

The geometric parameters of the dimples, such as depth, diameter, and density, are also critical in determining the lubrication performance. Some research mentioned that the positioning and depth of dimples have a direct influence on static and dynamic stability in journal bearings. In addition, Li et al., 2021 compared different bottom profiles of dimples (flat, curved, triangular, and chevron) and demonstrated that flat-bottom profiles enhanced load support more efficiently as in Figure 2. These findings emphasise that not only the depth but also the fundamental geometry of the dimple governs film pressure generation.

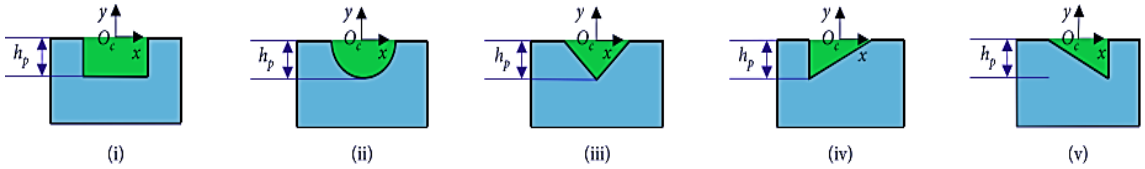

Figure 2: Bottom profiles of dimples (i) flat (ii) curved (iii) triangle (iv) backward chevron and (v) forward chevron (Li et al., 2021).

More advanced approaches have further considered the interaction between surface texturing and structural deformation. For instance, a study published in (Shinde and Chavan, 2020) that applied fluid–structure interaction (FSI) analysis to textured water-lubricated journal bearings, revealing that groove geometry and operating speed strongly affect film pressure, load capacity, and friction coefficient. Similarly, authors (Uddin et al., 2017; Wei et al., 2020) confirmed through numerical and experimental studies that dimple geometry, orientation, and distribution can significantly alter hydrodynamic film formation and wear resistance.

Overall, the literature suggests that the effectiveness of surface texturing is highly dependent on dimple depth, geometry, and distribution, as well as operating parameters such as bearing length. While many works have addressed the role of dimple geometry in hydrodynamic bearings, the influence of dimple depth under varying bearing dimensions and operating conditions remains a subject requiring further investigation. The aim of this study is to use a 3D CFD simulation in ANSYS to analyse how dimple textures affect the behaviour inside a journal bearing. This work focuses on how the dimple geometry interacts with the bearing L/D ratio and uses the realizable k–ε model to capture turbulence effects that are usually ignored.

2.0 EXPERIMENTAL PROCEDURE

In this paper, a typical 3-dimensional journal bearing model was developed using the ANSYS software. A few dimple shapes were designed on the journal bearing surface (circle, ellipse and square) with 0.5 mm depth. The lubricating oil used is hydraulic oil. Two types of bearing with

different length-to-diameter (L/D) ratios were tested in this study. Table 1 shows the parameters of the bearing based on the chart (Raimondi and Boyd, 1958) by assuming the bearing characteristics number, S was 0.14. The location of the maximum pressure, $\emptyset_{Pmax}$, was determined to be at 18.5° clockwise, as in Figure 3, which corresponds to the position of the dimples.

Table 1: Bearing Parameters

Parameters	**Descriptions**
Bearing length (mm)	100 and 55
Shaft length (mm)	100
Radial clearance (mm)	0.5
Attitude angle (°)	54
Position of minimum film thickness (°)	54

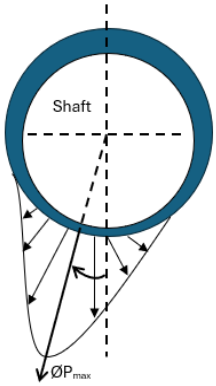

Figure 3: Bearing profile.

The first simulation was done on the plain surface bearing for both L/D types. The simulations were done in computational fluid dynamics (CFD) using ANSYS software combining fluid flow (FLUENT) and transient structural in coupling system simulation. Realizable k-epsilon (k-ε) model was used in FLUENT to consider the possible presence of fluid cavitation during simulation. The realizable k-ε was a combination of the Navier-Stokes equation and the turbulence model.

The bearing design was drawn in fluid flow (Fluent) as shown in Figure 4, then connected to transient structural, and both were combined in a coupling system model to complete the simulation process. In the fluid flow model, the parameters were set on meshing, such as in Figure 5, shaft speed, lubricant density and viscosity. Mathematical models that describe the motion of the fluid momentum, which is the Navier-Stokes equation as Equation (1), and the energy equation as Equation (2) for heat transfer. The tolerance for convergence was 1.0×10^{-6}, to avoid any inaccurate reading and to ensure the quality during the meshing. Besides that, the cavitation model used in this simulation was the Zwart-Gerber-Belamri model, and all the bubbles were assumed to be the same size and constant density to simplify the numerical simulation.

In transient structural and coupling systems, parameters such as load bearing and analysis duration (time step) were set, respectively. The governing equation for deformation in transient structural was used as Equation (3), Equation (4) and Equation (5). While in the coupling system model, the fluid domain and structure domain as Equation (6) and Equation (7) were used. In this,

kinematic (for displacement) and dynamic (for stress) boundary conditions were taken into consideration. The simulation parameters were shown in Table 2 to 5.

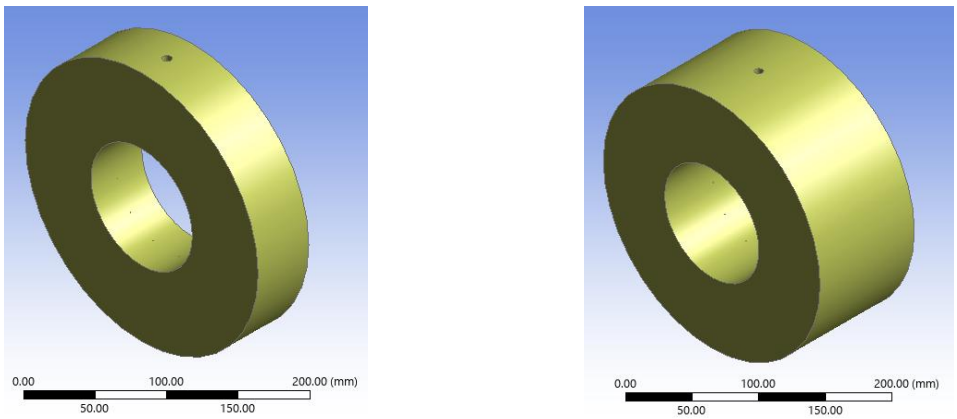

(a) (b)

Figure 4: Drawing of plain surface bearing with different length-to-diameter ratio (a) 0.5 and (b) 1.0.

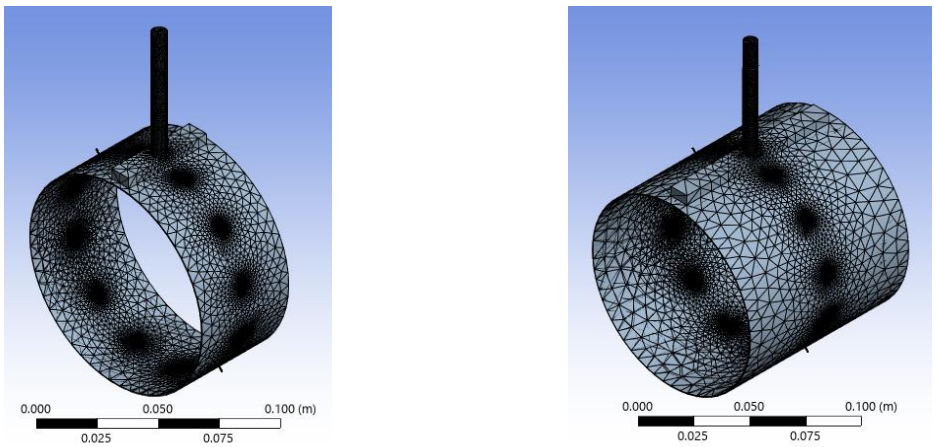

(a) (b)

Figure 5: Meshing profile for plain surface bearing with different length-to-diameter ratio (a) 0.5 and (b) 1.0.

$$\nabla . u = 0, \frac{\partial u}{\partial t} + \nabla . (uu) = -\nabla p + \mu \nabla^2 u + f \quad (1)$$

$$\nabla . \sigma = f \quad (2)$$

where, u is the displacement vector, σ is the stress tensor and f is the body force.

$$\frac{\partial \rho u}{\partial t} + \nabla . (\rho uu) = -\nabla p + \nabla . \tau + f \quad (3)$$

where, ρ is the fluid density, p is pressure, τ is the viscous stress tensor and f is the body force.

$$\frac{\partial(\rho E)}{\partial t} + \nabla.\left(u(\rho E + p)\right) = \nabla.(k\nabla T) + Q \quad (4)$$

where, E is total energy per unit mass, k is thermal conductivity, T is temperature and Q represents the heat sources.

$$\nabla.\sigma + f = 0 \quad (5)$$

$$\sigma = C:\epsilon \quad (6)$$

$$\epsilon = \frac{1}{2}(\nabla u + (\nabla u)^T) \quad (7)$$

where, σ is the stress tensor, f is the body force, C is the stiffness matrix, ϵ is the strain tensor and u is the displacement vector.

Table 2: Meshing parameters.

Meshing parameters	**Descriptions**
Span angle center sizing	Coarse
Transition sizing	Fast
Inflation option	Smooth transition
Smoothing quality	Medium
Transition ratio	0.272
Growth rate	1.2
Maximum layers	5

Table 3: Fluid flow (Fluent) parameters.

Fluid flow (Fluent) parameters	**Descriptions**
Shaft speed (rpm)	300
Lubricant density (kg/m^3)	860
Lubricant viscosity (kg/ms)	0.05848

Table 4: Transient structural parameters.

Transient structural parameters	**Descriptions**
Bearing load (kN)	10 and 20

Table 5: Coupling system parameters.

Coupling system parameters	**Descriptions**
Time step (s)	50
Iteration (times)	5

Next, the simulation was repeated on the bearing with a textured surface. For reference, the dimple design from (Wang et al., 2023) was used, and some modifications were made to the dimple design to obtain the best design of the dimple when put on the bearing surface. The

parameters of the dimple design were listed in Table 6 and Table 7. The dimples were placed on the bearing where the max pressure was located, as shown in Figure 6. Lastly, the results were analysed to determine the improvement made from having the dimple on the bearing surface in terms of the pressure.

Table 6: Dimple design parameters.

Parameters	**Descriptions**
Dimple shape	Square
Length (mm)	2
Dimple depth (mm)	0.5
Area ratio	5%

Table 7: Modification of dimple depth.

Parameters	**Descriptions**
Shape	Circle and ellipse
Diameter (mm)	2
Dimple depth (mm)	0.1, 0.2, 0.3, 0.4, 0.6, 0.7, 0.8, 0.9 and 1.0

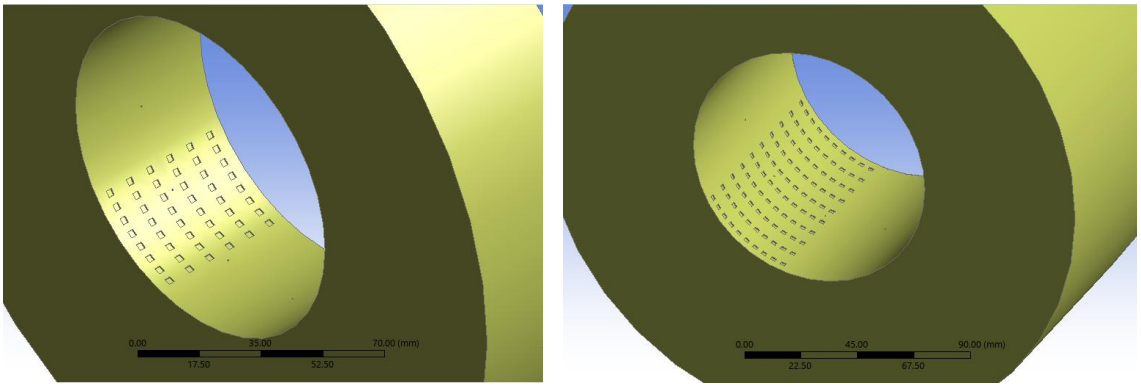

(a) (b)

Figure 6: Dimples location on the bearing surface for different length-to-diameter ratio (a) 0.5 and (b) 1.0.

3.0 RESULTS AND DISCUSSION

After the coupling system models were simulated, all the results were observed to see the pressure profile on the bearing surface. The results for different L/D ratio plain bearings were portrayed in Figure 7.

Figure 7 illustrates the pressure distribution within the journal bearing. It can be seen that the pressure is not evenly distributed but rather concentrated in specific locations for both types of bearings. The bearing's maximum pressure occurs in the lower-right zone (red region), while the minimum pressure is found on the opposite side (blue region). This pattern is compatible with the expected load direction, in which the applied radial load shifts the shaft to one side, causing an eccentricity and pressure build-up in the converging region.

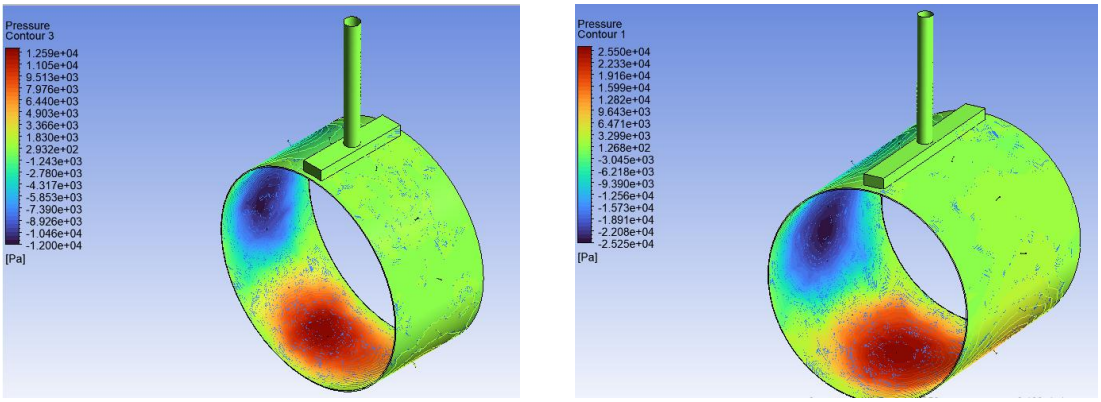

(a) (b)

Figure 7: Pressure contour for plain surface bearing with different L/D ratio (a) 0.5 and (b) 1.0.

The peak pressure for L/D ratios 0.5 and 1.0 was roughly at 12.5 kPa and 25.5 kPa, respectively, indicating the bearing's ability to handle the imposed load. However, negative pressure regions are observed, which may indicate a possibility of cavitation in the diverging zone of the fluid film. Such events are essential because they can affect bearing stability and lubrication performance.

The pressure distribution reveals that the bearing surface is not uniformly loaded, with concentrated high-pressure zones holding the majority of the imposed load. This behaviour is consistent with theoretical predictions based on Reynolds' equation, which state that the pressure maximum occurs somewhat behind the applied load's line of action.

Following completion of the simulation, Figure 8 shows the pressure contour on the various bearing surface conditions (dimple texturing) at 10 kN load and 300 rpm speed. When dimples are added (Figures 8a to f), the pressure distribution varies significantly depending on the shape of the texturing. Figures 8a, 8c, and 8e demonstrate a more dispersed pressure field, with lower peak values but more evenly distributed pressure, which may aid in enhancing stability and minimizing localised wear. The peak pressure is roughly at 10 to 12 kPa for shorter bearing length. In other cases, such as Figures 8b, 8d, and 8f, the dimples enhance peak pressure while broadening the high-pressure zone, indicating an increase in load-carrying capability. The peak pressure recorded was around 23 to 25 kPa, slightly higher compared to the L/D of 0.5 for longer bearing length. In some designs, the presence of dimples has an impact on journal bearing performance. This can help minimise cavitation concerns, but improperly placed dimples might worsen the effect. An optimum dimple design can improve hydrodynamic performance, balance load support, and reduce potential difficulties like cavitation and unequal stress distribution. Figure 9 and Figure 10 show the pressure profile for different bearing conditions.

Figure 9 illustrates the pressure profiles of bearings with various dimple texturing shapes (plain, circle, ellipse, and square) under a load of 10 kN at a speed of 300 rpm on different L/D ratios (0.5 and 1.0). At L/D 0.5, the range of peak pressure was 10 to 13 kPa; at L/D 1.0, the range of peak pressure increased to 23 to 27 kPa. While Figure 10 illustrates the pressure profiles of bearings with various dimple texturing shapes (plain, circle, ellipse, and square) under a load of 20 kN at a speed of 300 rpm on different L/D ratios (0.5 and 1.0). The peak pressure for both L/D ratios was observed to have no significant changes compared to operating at a 10 kN load.

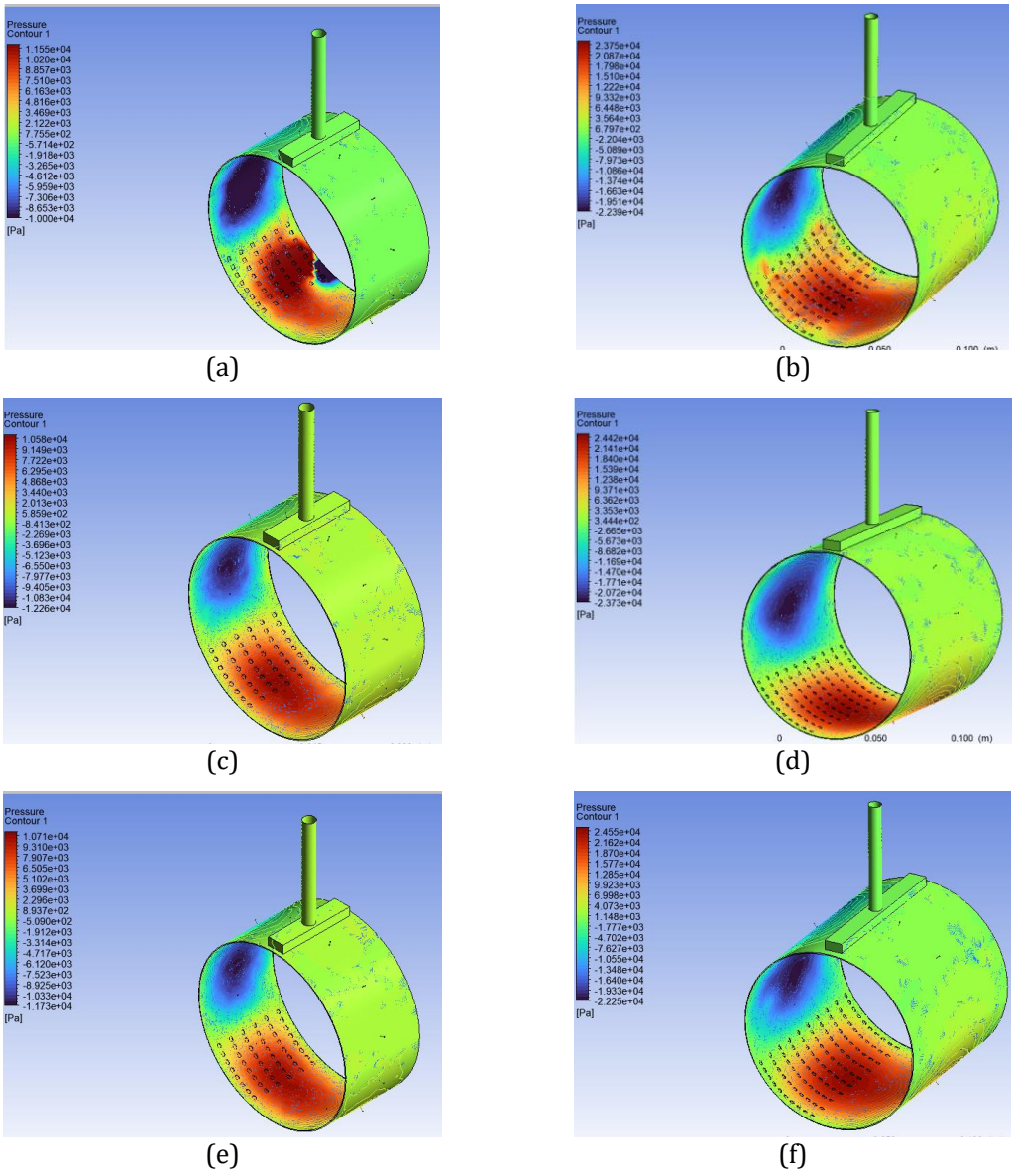

Figure 1: Pressure contour on the various bearing surface conditions (dimple texturing) with different length-to-diameter ratio at load 10kN and speed of 300 rpm (a) Square L/D 0.5, (b) Square L/D 1.0, (c) Circle L/D 0.5, (d) Circle L/D 1.0, (e) Ellipse L/D 0.5, and (f) Ellipse L/D 1.0.

The hydrodynamic pressure generated within a journal bearing directly contributes to its load-carrying capacity, particularly in the converging wedge region near the peak pressure zone (approximately 180° - 210°) (Fuad et al., 2025; Gahir et al., 2024). Although a plain bearing surface may exhibit a higher peak pressure, its rise and drop are sharp, resulting in a narrow positive-pressure region and deeper negative pressure in the divergent zone, which increases the likelihood of cavitation and film instability.

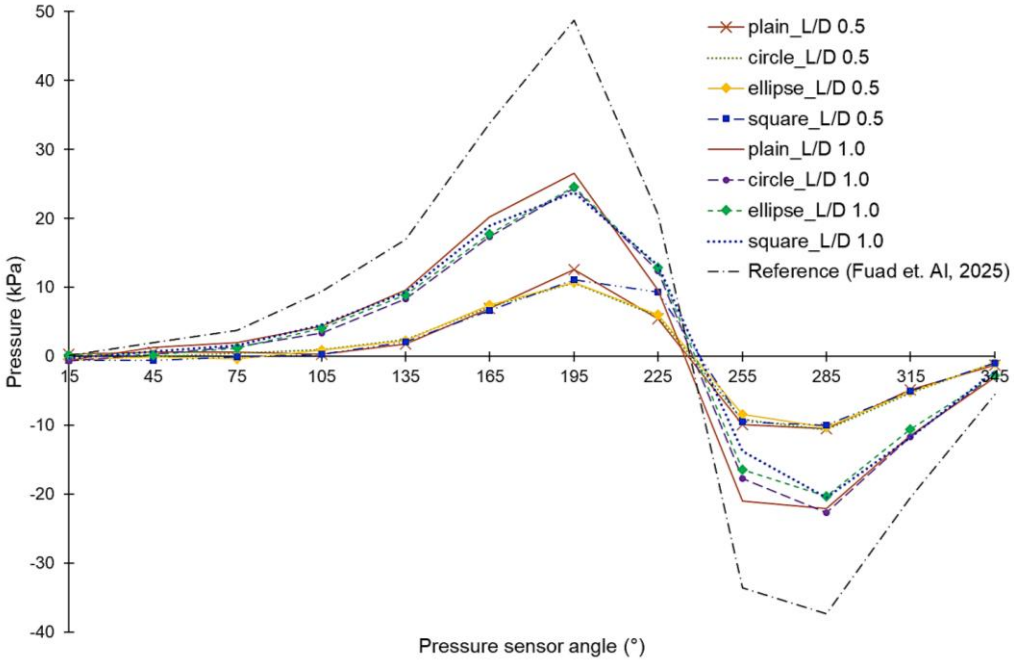

Figure 9: Pressure profile for different surface conditions at 300 rpm and 10kN.

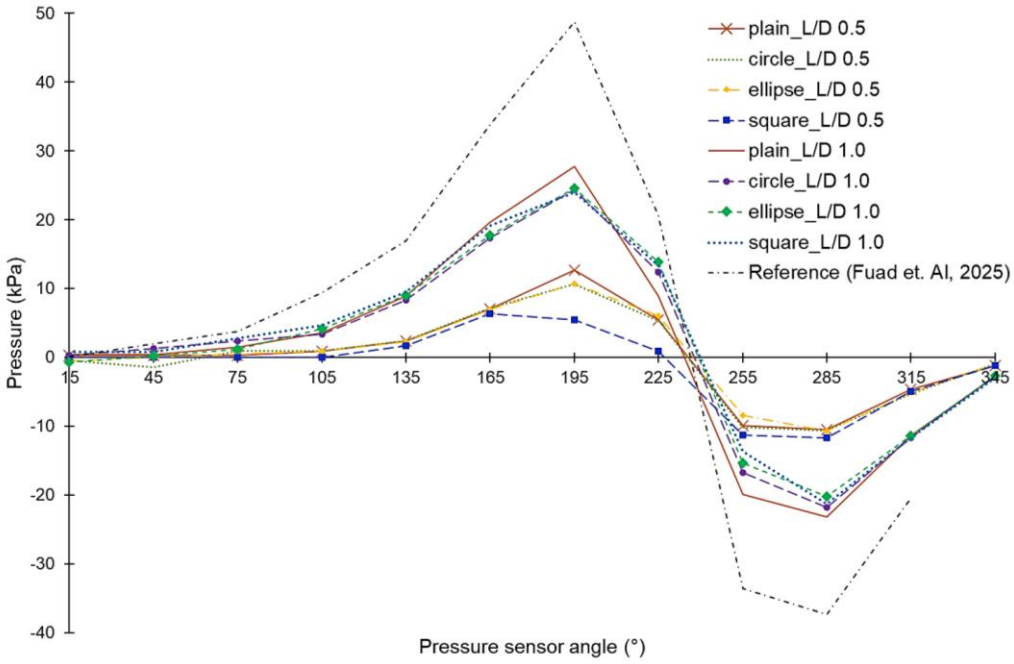

Figure 10: Pressure profile for different surface conditions at 300 rpm and 20kN.

In contrast, dimple-textured surfaces, especially those with circular and elliptical shapes, produce a slightly lower peak pressure but maintain a wider positive pressure distribution and mitigate negative pressure drops. This leads to enhanced lubrication stability, increased film thickness, and an overall enhancement of the effective load-carrying area beneath the pressure curve (Shen and Khonsari, 2013; Liu et al., 2020; Wang et al., 2023). Therefore, textured bearings generally outperform plain bearings in terms of lubrication performance.

Square dimples, particularly at a lower L/D ratio (0.5) at load 20 kN, show reduced pressure enhancement due to sharp-corner geometry, which induces flow separation and energy loss (Sahu et al., 2025). Consequently, square dimples provide less hydrodynamic benefit compared to circular and elliptical textures, specifically on bearings with L/D 0.5 at a load of 20 kN.

After analysing the pressure profiles for various surface textures, it is crucial to examine the influence of dimple depth, since this parameter has a significant impact on the hydrodynamic performance of textured bearings. When the dimples are excessively shallow, their influence on pressure enhancement is negligible, and the performance is comparable to a flat surface. On the other side, raising the dimple depth increases the micro-cavities' ability to generate more hydrodynamic pressure, which improves load support and can reduce friction by maintaining a thicker lubricant film, which is called a lubricant reservoir (Roy et al., 2018).

However, beyond an optimal depth, the pressure distribution becomes less uniform, and excessive negative pressure zones may form, increasing the risk of cavitation and instability. This may also result in higher localised shear stress, leading to increased friction and accelerated wear. Therefore, dimple depth must be carefully optimised; a moderate depth provides a balance between improved pressure generation and stable lubrication, whereas excessive depth can have a detrimental effect on both friction and wear (Kasem et al., 2018).

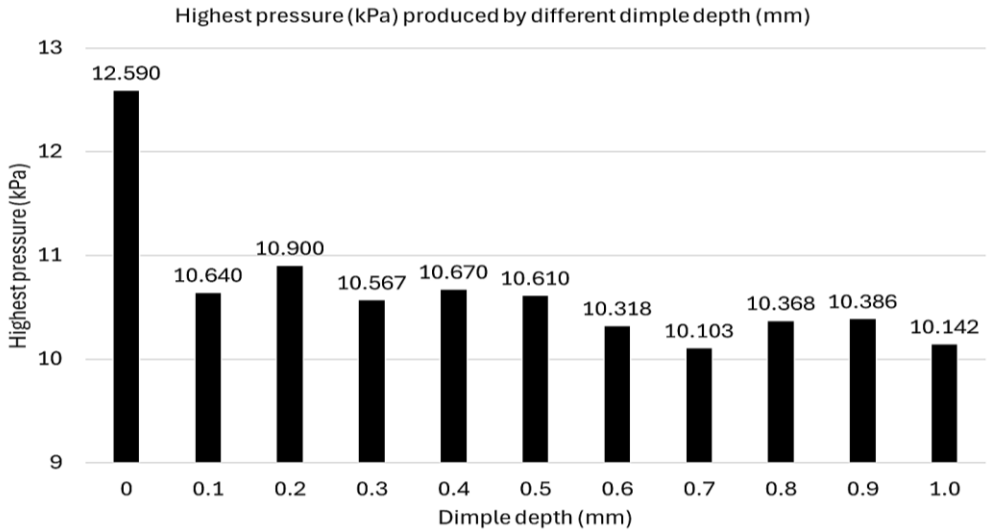

Figure 11: Highest pressure (kPa) produced by different dimple depth (mm).

The bar graph in Figure 11 depicts the maximum pressure (in kPa) produced at different dimple depths (in mm), demonstrating a strong relationship between surface texture and pressure generation. The highest pressure of 12.590 kPa is observed at a dimple depth of 0 mm, indicating a flat surface that creates the highest pressure. Introducing dimples results in a

significant drop in pressure, with even a minor dimple depth of 0.1 mm lowering it to 10.640 kPa. Beyond this point, from 0.2 mm to 1.0 mm, pressure readings vary slightly between 10.103 kPa and 10.900 kPa, with no discernible upward or downward trend. The lowest pressure was recorded at 0.7 mm with 10.103 kPa. Overall, the graph shows that, while smooth surfaces provide the most pressure, the addition of dimples, even at minimum depths, effectively reduces the pressure.

4.0 CONCLUSION

The numerical analysis confirms that both the L/D ratio and surface texture significantly affect the hydrodynamic behaviour of journal bearings.

- Bearings with an L/D ratio of 0.5 generated approximately 50% lower pressure compared to those with an L/D ratio of 1.0.
- Surface texturing improved pressure reduction by more than 15%, with the circular dimple exhibiting the most effective performance. A 0.7 mm dimple depth was identified as the optimum configuration, achieving about 19% greater pressure reduction than the plain surface in this study.

In conclusion, the study emphasises that the dimple depth and the L/D ratio can significantly enhance hydrodynamic bearing performance by improving pressure generation, reducing surface friction and promoting more stable lubrication conditions.

REFERENCES

Cohen, I., & Goltsberg, R. (2023). Partial surface texturing in hydrodynamic lubrication: A CFD-based investigation. Lubricants, 11(9).

Fuad, N. N. N. A., Ahmad, M. A., & Ghani, J. A. (2025). CFD analysis of textured journal bearing for performance parameters. Jurnal Tribologi, 46, 1–12.

Gahir, G. S., Pal, S., & Matharu, S. (2024). CFD evaluation of steady and fluctuating depth dimpled textures impacting the efficiency of hydrodynamic journal bearings. Journal of the Brazilian Society of Mechanical Sciences and Engineering, 44(3), 13814–13829.

Kasem, H., Stav, O., Grützmacher, P., & Gachot, C. (2018). Effect of low depth surface texturing on friction reduction in lubricated sliding contact. Lubricants, 6(3), 1–10.

Khonsari, M. M., & Booser, E. R. (2017). Applied tribology: Bearing design and lubrication (3rd ed.). John Wiley & Sons.

Kligerman, Y., Etsion, I., & Shinkarenko, A. (2005). Improving tribological performance of piston rings by partial surface texturing. Journal of Tribology, 127(3), 632–638.

Kong, H., Gu, C., Zhang, D., & Wu, L. (2025). Topology optimization of textured journal bearings. Lubricants, 13(6), 1–16.

Li, P., Zeng, F., Xiao, S., Zhen, D., Zhang, H., & Shi, Z. (2021). Effects of texture bottom profile on static and dynamic characteristics of journal bearings. Shock and Vibration, 2021, 1–12.

Liu, W., Ni, H., Wang, P., & Chen, H. (2020). Investigation on the tribological performance of micro-dimples textured surface combined with longitudinal or transverse vibration under hydrodynamic lubrication. International Journal of Mechanical Sciences, 174.

Liu, Y., Gao, G., Yin, Z., Jiang, D., & Ding, N. (2021). The design of eccentricity ratio, relative clearance and length-to-diameter ratio of water-lubricated journal bearings under different working conditions. Journal of Physics: Conference Series, 1948(1).

Marey, N. (2019). An experimental investigation of hydrodynamic journal bearing with different oil grades. Port-Said Engineering Research Journal, 23(2), 46–54.

Raimondi, A. A., & Boyd, J. (1958). A solution for the finite bearing and its application to analysis and design. ASLE Transactions, 1(1), 159–209.

Roy, T., Choudhury, D., & Murphy, B. P. (2018). Tribological influences of micro texture on surface interfaces: A review. Tribology of Materials, 1(1), 1–12.

Sahu, V. K., Shukla, P. C., & Gangopadhyay, S. (2025). Development of surface textures using micro-milling operation for improved tribological characteristics of aluminium alloy. International Journal of Advanced Manufacturing Technology, 136(1), 367–382.

Sharma, S., & Awasthi, R. K. (2018). Effect of aspect ratio on the performance and stability of hydrodynamic journal bearings. Mechanics and Mechanical Engineering, 22(1), 153–170.

Shen, C., & Khonsari, M. M. (2013). Effect of dimple's internal structure on hydrodynamic lubrication. Tribology Letters, 52(3), 415–430.

Shinde, A. B., & Chavan, S. P. (2020). Parametric investigation of surface texturing on performance characteristics of water lubricated journal bearing using FSI approach. SN Applied Sciences, 2(1), 1–15.

Tala-Ighil, N., Fillon, M., & Maspeyrot, P. (2011). Effect of textured area on the performances of a hydrodynamic journal bearing. Tribology International, 44(3), 211–219.

Uddin, M. S., Ibatan, T., & Shankar, S. (2017). Influence of surface texture shape, geometry and orientation on hydrodynamic lubrication performance of plane-to-plane slider surfaces. Lubrication Science, 29(3), 153–181.

Wang, Y., Jacobs, G., König, F., Zhang, S., & von Goeldel, S. (2023). Investigation of microflow effects in textures on hydrodynamic performance of journal bearings using CFD simulations. Lubricants, 11(1).

Wei, Y., Tomkowski, R., & Archenti, A. (2020). Numerical study of the influence of geometric features of dimple texture on hydrodynamic pressure generation. Metals, 10(3).